Quantum condensation of liquid ^{4}He

2003 J. Phys.: Condens. Matter 15 4717

(http://iopscience.iop.org/0953-8984/15/27/306)

INSTITUTE OF PHYSICS PUBLISHING JOURNAL OF PHYSICS: CONDENSED MATTER

J. Phys.: Condens. Matter **15** (2003) 4717–4738 PII: S0953-8984(03)60159-1

Quantum condensation of liquid ^{4}He

Mark Brown and Adrian F G Wyatt

School of Physics, University of Exeter, Exeter EX4 4QL, UK

Received 27 February 2003
Published 27 June 2003
Online at stacks.iop.org/JPhysCM/15/4717

Abstract

We present experimental results on the condensation of ^{4}He atoms on the surface of liquid ^{4}He. We show that there is quantum condensation with the creation of phonons and R^+ rotons in one-to-one processes as atoms go into the Bose–Einstein condensate. These phonon and R^+ roton signals can be recognized by their time of flight, their angular distribution and their dependence on the ambient temperature. Condensing atoms also create ripplons with a high probability. We derive rate equations for the growth of the ripplon density and the ripplon decay by the creation of bulk phonons. During the atom pulse a dynamic equilibrium is established. The low-energy phonons that are created by ripplon–ripplon scattering can easily be detected and distinguished from the phonons created by quantum condensation.

From measured data, estimates are made of the probabilities of creating phonons, R^+ rotons and ripplons in condensation processes as well as estimates of the quantum evaporation probabilities of phonons and rotons.

We clearly detect R^+ rotons directly with a bolometer in the liquid ^{4}He and show why the signal of R^+ rotons is obscured by the low-energy phonon signal when both the source and detector are in the liquid helium. Values of the Kapitza conductance for the Zn bolometers are derived.

1. Introduction

In this paper we describe the processes that follow a ^{4}He atom condensing onto the free surface of liquid ^{4}He. As this is the inverse process of evaporation, we might expect that excitations are produced in the liquid. We know that all three types of excitations in liquid ^{4}He can cause quantum evaporation [1–3]. High-energy phonons, with energy $\hbar\omega/k_B > 10$ K, and R^+ rotons readily eject ^{4}He atoms from the surface of liquid ^{4}He. R^- rotons also create free atoms, but with a much lower probability, and so are much harder to detect.

The characteristics of quantum evaporation are well established [4]. First it is a one-to-one process: one excitation of the liquid ^{4}He is annihilated at the free surface and one free atom is created from the Bose–Einstein condensate. Second, energy is conserved. The energy of the

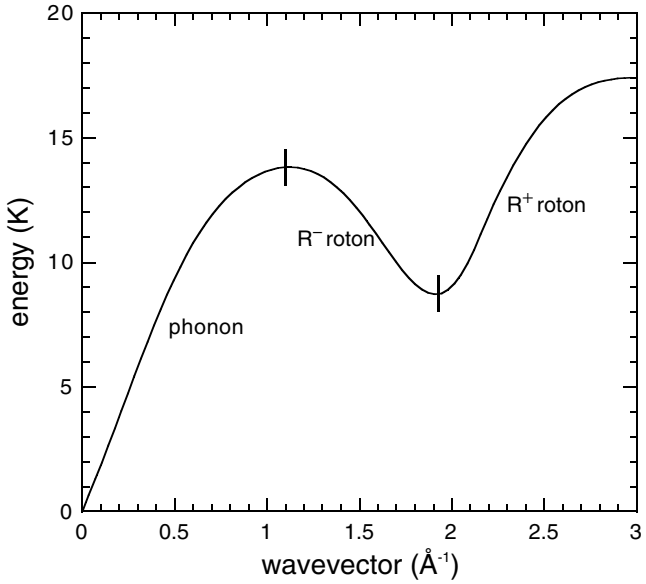

Figure 1. The dispersion curve for liquid ^{4}He showing the phonon, R^- roton and R^+ roton regions.

excitation goes in overcoming the binding energy of the atom in the liquid, $\epsilon_B = 7.16$ K, and the remainder is taken away as kinetic energy of the free atom, i.e.

$$\hbar\omega = \epsilon_B + p_4^2/2m_4 \tag{1}$$

where p_4 is the momentum and m_4 the mass of the free atom. The third characteristic is that the parallel component of the wavevector is conserved: i.e.

$$q_\parallel = k_\parallel \tag{2}$$

where q and k are wavevectors of the excitation and atom, respectively. This arises from the translational invariance of the free liquid surface. The energy and wavevectors of an excitation are related through the dispersion curve. This is a continuous curve which is divided into three regions: phonons in the range $0 < q < 1.1$ Å^{-1}, R^- rotons in the range $1.1 < q < 1.92$ Å^{-1} and R^+ rotons with $q > 1.92$ Å^{-1}, see figure 1.

Compared to quantum evaporation, there has been much less work done on condensation mainly because the experimental results are more difficult to interpret. Also the signals are smaller due to the need to use a low flux of atoms so that flux-independent results are obtained. Higher fluxes create too many ripplons which spoil the translational invariance of the surface. The low sensitivity of the bolometer in the liquid to phonons and rotons also makes the signals small.

There are several fundamental questions concerning atom condensation. First, are there one-to-one processes, atom $\rightarrow$ phonon, atom $\rightarrow$ R^+ roton and atom $\rightarrow$ R^- roton, and if so what is their probability? Second, are there other processes which are impossible in evaporation experiments, such as one atom creating two bulk excitations? Third, what is the role of ripplons which are copiously produced in condensation? Furthermore there is the question of whether rotons can be detected in the liquid ^{4}He by a solid detector, such as a bolometer.

The first measurements of the signals in the liquid ^{4}He, created by a beam of condensing atoms at 42° incidence [5], showed a very broad angular distribution which was interpreted as one atom creating simultaneously a bulk excitation and ripplons. This interpretation became

redundant when the angular distribution was measured with a higher angular resolution, achieved by reducing the incident atom flux [6]. It was clear that the main beam of excitations, created in the liquid ^{4}He, is at the angle expected for one atom creating one R^+ roton. The reason for the low angular resolution at high atom fluxes is that the translational invariance of the surface is broken by ripplons. The bulk excitations are then not created in narrow beams at an angle, given by equation (2), relative to the mean plane of the surface. This spoiling of the surface has been studied [7].

Atom beams incident on the free surface of liquid ^{4}He have some probability of being reflected as well as condensing. Edwards *et al* [8–10] have shown that the reflectivity is a strong function of the perpendicular component of the wavevector, $k_\perp$. This is due to quantum reflection depending on the relative size of the perpendicular component of the wavelength of the atom and the distance over which the surface potential changes. The surface appears more abrupt for longer wavelengths and so gives a higher reflectivity. At normal incidence, for a typical atom with energy $\approx$4 K, the reflectivity is very small, $\approx 10^{-5}$, and most of the atoms condense. The measured reflectivity agrees with that calculated. The detected reflectivity is specular, which shows no other excitation is involved as another excitation would carry away energy and momentum. The specular reflectivity is reduced if too many ripplons are created. This happens if the incident atom beam flux is too high, or if a second atom beam is used to spoil the surface by creating ripplons [7].

However, at large angles to the normal, around 80°, it is found for some particular atom energies that the reflectivity is increased [11]. At these energies it is impossible to create bulk phonons or rotons and conserve energy and the parallel component of the wavevector. Now there are several channels for the interaction between an atom and the liquid helium and if one channel closes, then the probabilities for the other possible channels increase. In particular if a transmission channel closes then the reflectivity channel increases. The size of the reflectivity change indicates that $>1.5\%$ of the incident atoms create phonons and $>3\%$ create rotons. However, it must be remembered that the phonon energy is $\approx$8.4 K which is lower than that used for quantum evaporation, and the roton created is at the roton minimum which corresponds to zero group velocity and so again these rotons are not used in quantum evaporation. We shall find that the probability for creating large wavevector R^+ rotons is much higher than 3% but for phonons it is $\sim 1\%$.

The broad picture presented in this paper is that the atoms in an atom beam at 45° incidence and typical energies 2–6 K mostly condense and only a very small fraction of the atoms are specularly reflected. About 0.6 of the beam creates ripplons and about 0.4 creates bulk excitations in one-to-one processes. These are mainly rotons; relatively few phonons are created. Many more phonons are produced by the decay of the ripplons. It is against this background that we present our results. In section 2 we describe the experiment. In section 3 we present the measured angular distribution and its interpretation which is justified in the rest of the paper. In section 4.1 we consider the phonons that are created in the bulk liquid by one-to-one processes and in 4.2 the probability of these processes. This will lead on to section 4.3 where we analyse the creation of ripplons and their decay into bulk phonons. In section 4.4 the power dependency of these processes is discussed. In section 5.1 we discuss the creation of R^+ rotons and in 5.2 why they give a detectable signal on the bolometer. Conclusions are drawn in section 6.

2. The experiment

The apparatus is the same as that used previously in the quantum evaporation experiments and is described in detail in [4]. A schematic diagram of the arrangement is shown in figure 2.

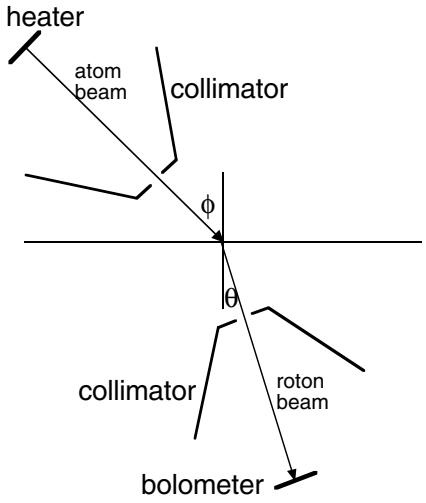

Figure 2. Schematic drawing of the apparatus. The atom and roton path lengths are 6.5 and 6.6 mm respectively.

A 1 mm^2 gold heater, on glass, is pulse heated for typically 2 μs. This heats the liquid ^{4}He film covering the heater. Helium atoms are evaporated and are collimated into a beam which is directed at the free liquid surface. The collimator aperture, cut in a mica sheet, is 0.4 mm $\times$ 1.0 mm with the long dimension parallel to the axis of rotation. The heater is 4.5 mm from the collimator and 6.5 mm from the liquid surface. The path length from the liquid surface to the bolometer is 6.6 mm and there is a similar collimator in this path. The bolometer is superconducting Zn in a magnetic field which is kept at a constant temperature, $\sim$0.35 K, and hence constant resistance R_0, by a fast electronic feedback circuit [12–14]. To a reasonable approximation the detected power is given by $W = V_0\delta V/2R_0$, where $V_0/2$ is the quiescent voltage across the bolometer and δV is the signal.

Both the heater and bolometer can be rotated independently, in a vertical plane, by two superconducting stepper motors. The angular positions are determined by potentiometers to within $\approx$1°. However, we estimate that the systematic uncertainty is $\approx$3°. For most of the data reported here the atom beam is at an angle of incidence of 45° to the normal. The liquid level is set to within 0.1 mm of the rotation axis using a Karma resistance wire of 15 μm diameter positioned at the required level [15]. The atom signal from the pulse-heated wire disappears when the liquid level reaches the wire. Isotopically pure ^{4}He is used to prevent ^{3}He contamination of the surface. The temperature of the liquid helium is measured with a calibrated Ge thermometer and unless otherwise stated all measurements were made at ambient temperatures of $\approx$80 mK. The input heater power and pulse length have to be carefully chosen for some of the signals as they disappear into the noise if the input energy is too high.

3. The angular distribution

Representative signals created by a pulsed atom beam at an angle of incidence of 45°, at different bolometer angles, are shown in figure 3. The peak heights of these signals vary considerably. The largest is $\approx$30 times that of the smallest. At angles around 15°, the signal is large and has a relatively short duration. At this angle an atom can create a R^+ roton in a one-to-one process. At angles around 45°, the signal is small and dispersed in time. We shall see that this signal arises from ripplons created by the condensing atoms. At angles around

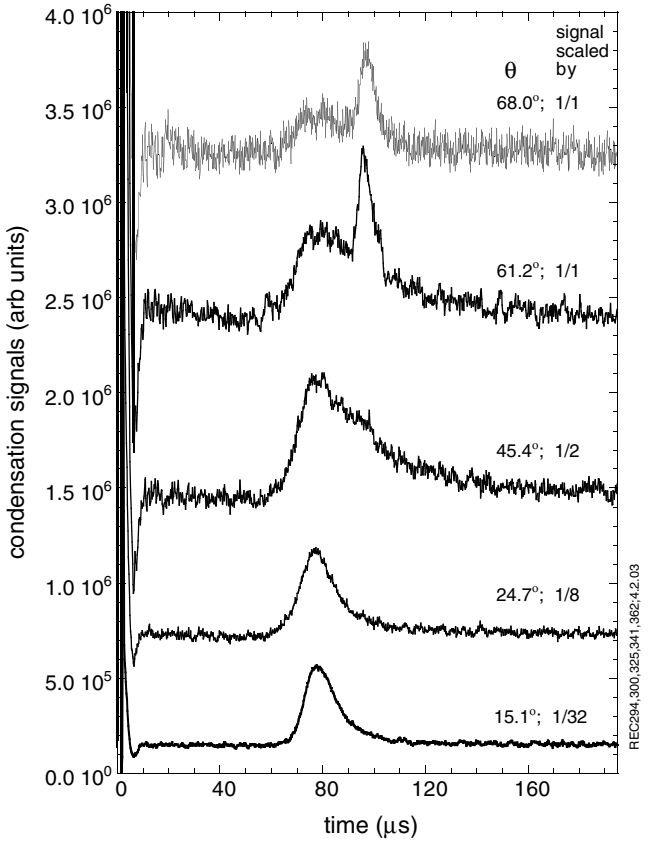

Figure 3. Typical signals at different angles θ. $\phi = 45°$ and the heater pulse is 8 mW and 2 μs. The signals are scaled vertically by the factors shown and are offset vertically.

61.2° the dispersed signal has a narrow peak superimposed on it. At this angle an atom can create a phonon in a one-to-one process. This sharp signal starts at 92 μs which is the time expected for this process. By 68°, both these signals have decreased to half their size at 61.2°.

In figure 4 we show the measured angular distribution created by a pulsed atom beam at an angle of incidence of 45°. To show the energy as a function of bolometer angle, signals similar to those in figure 3 are integrated over time ($50 < t < 190$ μs) for this plot. The heater pulse is 8 mW for 2 μs which is small enough for the angular dependence to be independent of power, except for quantum condensed phonons which are a maximum at this power. These power-dependent effects are described in section 4.4.

There are three components to the angular distribution. The largest peak, with a maximum at 12°, is at the angle expected for one atom creating one R^+ roton. The middle-size peak, around 50°, does not correspond to the angle of any one-to-one process. We shall argue that it is due to low-energy phonons created by ripplons. The smallest peak, around 60°, has to be expanded 10 times to show on the same scale as the other two peaks. The angle and the time of flight of this peak identify it as the one atom to one phonon process with the phonon energy >10 K.

There is no sign of any signal that can be ascribed to one atom to one R^- roton process. This signal should be around angles of $-20°$. However, we should not be surprised that this signal is absent as we found in quantum evaporation that one R^- roton to one atom process

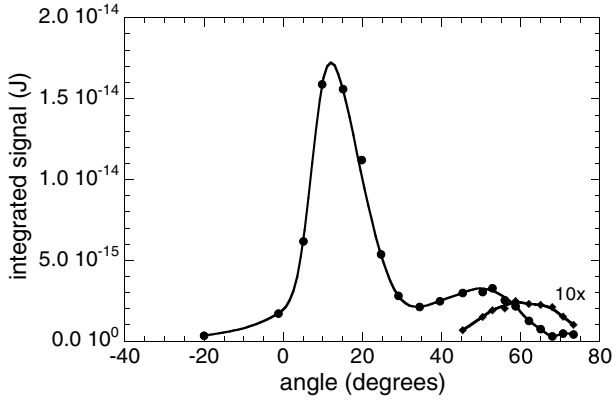

Figure 4. The time-integrated signal from condensing atoms as a function of bolometer angle. The diamonds are from integration over the narrow peak, see figure 3. The atom beam has an angle of incidence $\phi = 45°$. The heater pulse is 8 mW for 2 μs.

has a probability which is two orders of magnitude lower than that of the one R^+ roton to one atom process [16].

4. Atom to phonon processes

4.1. One atom to one phonon

We now consider the sharp peak which is shown in figure 3 at angles of 61.2° and 68.0°. We identify this with the one atom to one phonon process with energy and parallel momentum conserved at the free liquid surface. There are three characteristics that lead to this conclusion. They are the time of flight, the angular distribution, and the dependence on the ambient temperature of the liquid helium which causes scattering. We consider these in turn.

The incident atom flux has a range of energies, ϵ_a, so we might expect a range of phonons to be created in one-to-one processes, with energies $\epsilon_p = \epsilon_a + \epsilon_B$ where $\epsilon_B = 7.16$ K is the latent heat per atom. The behaviour of the phonons is quite different depending on whether ϵ_p is greater than, or ϵ_c is less than or equal to, 10.0 K. If $\epsilon_p < \epsilon_c$, then the created phonon will spontaneously decay by the three phonon process (3pp). This happens very rapidly with the inverse lifetime, given by $(u+1)^2 k_B^5 \epsilon_p^5 / 240\rho\pi\hbar^4 c^5$, [17], where we have used $k_B\epsilon_p/\hbar = \omega = cq$ and u, ρ and c are the Gruneisen constant, the density and the velocity of sound, respectively, for liquid helium. After a path length of 6.6 mm, these phonons successively decay to $\epsilon_p \approx 0.5$ K energy and are spread over a cone of half angle ≈27° [18]. The effect of spreading the energy over such a large cone angle is that the flux on the bolometer at any angle is very low. Also low-energy phonons create a much smaller signal as they have a much lower transmission into the bolometer than the high-energy phonons. The probability is down by a factor ≈10 [19, 20].

The signal from these phonons is also reduced as their time of arrival is very dispersed. This is due to the range of atom energies $\epsilon_a < (\epsilon_c - \epsilon_B)$ which causes the atom flux to be dispersed in time. The combined effects of space and time dispersion and the low detection probability make these phonons undetectable even though we know where to look for their fastest signal. For an atom with $\epsilon_a = (\epsilon_c - \epsilon_B) = 2.84$ K travelling over 6.5 mm and for phonons travelling at the ultrasonic velocity over 6.6 mm, the time is $59.8 + 27.3 = 87.1$ μs. There is no sign of such a signal at this time.

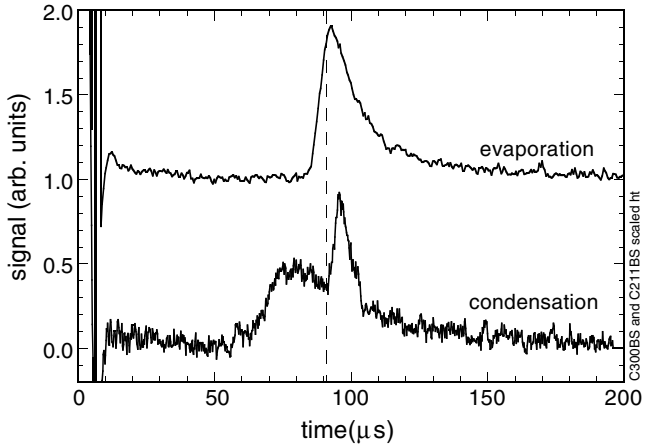

Figure 5. Comparison of an evaporation and a condensation signal. The vertical line at 92 μs is at the calculated time for 2.84 K atoms and 10 K phonons. The quantum evaporation signal arives faster because some of the path in the liquid ^{4}He is covered by faster low-energy phonons.

The situation is completely different for higher energy atoms. Those atoms with $\epsilon_a > 2.84$ K create phonons with $\epsilon_p > \epsilon_c = 10.0$ K which are completely stable against spontaneous decay [21–23]. So once created, high-energy phonons propagate to the bolometer ballistically, at their group velocity. These phonons only have an angular spreading due to the geometry of the collimation, heater and bolometer. Also there is little time dispersion because the change in atom velocity with energy ϵ_a is largely compensated by the change in phonon group velocity with energy ϵ_p, i.e. the faster atoms create slower phonons. The much smaller angular spreading and the small time dispersion mean that these phonons are in a more intense flux. This, with the higher bolometer sensitivity to these phonons, makes them detectable.

The fastest time for this process is for atoms with $\epsilon_a = 3.9$ K and the corresponding phonons with $\epsilon_p = 11.1$ K and group velocity 169 m s^{-1}. This gives a time of 92 μs. This agrees very well with the leading edge of the signal as is shown in figure 5. Also shown is the signal for quantum evaporation with the same path lengths. The faster leading edge is due to the high-energy phonons being created from the faster low-energy phonons just in front of the free surface of the liquid helium [18, 24].

The angular distribution of the sharp phonon signal is shown in detail in figure 6. The time-integrated signal is found by interpolating the broad signal in figure 5 underneath the sharp signal and then integrating the sharp signal from 90 to 110 μs. At $>70°$ the signal arises from phonons with $\epsilon_p = 10$ K and atoms at angles of incidence $>45°$ but within the collimation. Phonons with a higher energy give signals at smaller angles.

The dependence of the sharp signal on the ambient temperature of the liquid ^{4}He, [26], confirms its assignment as a one atom to one phonon process. In figure 7 we show the signal at $\theta = 61.2°$ at three temperatures. We see that the sharp signal has nearly disappeared by 147 mK and at 192 mK there is no sign of it. This indicates that the excitations that cause the sharp signal are ballistic high-energy phonons which are strongly scattered by the ambient thermal phonons at $T > 0.1$ K but are ballistic at $T < 80$ mK. This is characteristic behaviour of high-energy phonons, $\epsilon_p > \epsilon_c = 10$ K, and is markedly different to the behaviour of low-energy phonons, $\epsilon_p \approx 1$ K and rotons. Fast R^+ roton signals are attenuated by a factor of $\approx$0.5 at 150 mK compared to their low-temperature value but slow R^+ rotons are detectable at 300 mK [27]. Low-energy phonons are only weakly attenuated at 300 mK.

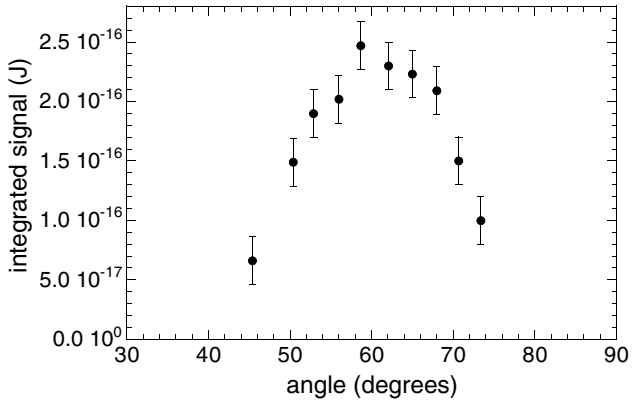

Figure 6. The one atom to one phonon time-integrated signals as a function of angle θ. $\phi = 45°$ and the heater pulse is 8 mW and 2 μs.

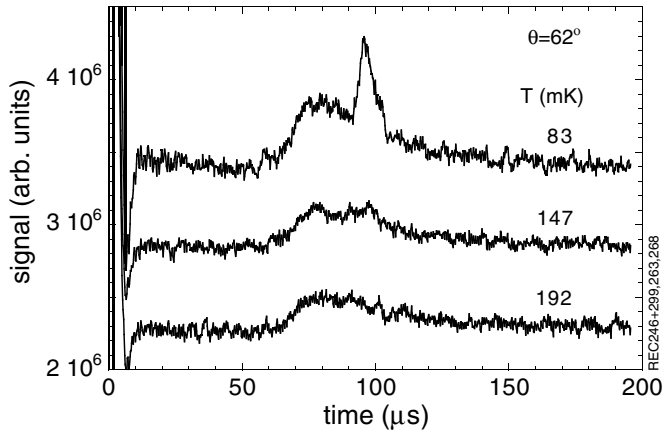

Figure 7. Condensation signals at various temperatures. $\phi = 45°$, $\theta = 62°$ and the heater pulse is 8 mW and 2 μs.

All the evidence indicates that the sharp signal, which broadly peaks around 60°, is due to high-energy phonons which are created by condensing atoms in one-to-one processes. We presume that phonons with energy <10 K are also created in one-to-one processes but their flux is too low to be detected. The probability of directly creating phonons in quantum condensation process is very low, which we now quantify.

4.2. The probability of the atom–phonon process

In this section we estimate the probability, p_{pa}, of a high-energy phonon, $\epsilon_p > 10$ K, evaporating an atom in a one-to-one process, and the probability, p_{ap}, of a condensing atom creating a high-energy phonon in a one-to-one process. It should be recognized that many of the values that we need are not known to within factors of two; nevertheless it is useful to make the best estimates that are currently possible as p_{pa} has been grossly overestimated [25] and it has been argued that $p_{ap} = p_{pa}$ when there are only one-to-one processes between atoms, phonons, R^+ rotons and R^- rotons, see equation (2) in [28].

We take a quantum evaporation experiment in which there are no collimators [29]. This is done because the high-energy phonons are strongly beamed in the direction normal to the heater, which means that any collimation must be aligned with the beam, to within a degree, for the peak signal to pass through. (We can use this property to show that the heater collimation used in the condensation experiments was indeed aligned to this accuracy.) The distance between the heater and bolometer is 13.1 mm and the liquid path length 8.1 mm. The heater pulse is 10 mW and 300 ns, i.e. an input energy of $E_h = 3.0 \times 10^{-9}$ J. The time-integrated energy detected in the bolometer is $E_b = 4.2 \times 10^{-14}$ J. From recent angular measurements of the low- and high-energy phonons emitted by a heater, using similar heater pulses [31], we estimate that $f_h = 0.31$ of the heater energy gets converted to high-energy phonons. This factor has an uncertainty associated with the extrapolation of the wings of the data to $\pm 90°$. Again from the angular measurements and the area of the bolometer, we estimate the fraction of the high-energy phonon beam that evaporates atoms which reach the bolometer is $f_g = 2.0 \times 10^{-2}$. This includes a factor of 1.18 increase in detected atoms due to the refraction of the atoms towards the normal. The two factors f_h and f_g are not independent of each other; in fact their product has less uncertainty than the factors have separately. Essentially all the atoms that land on the helium film, which covers the bolometer, condense and we assume that all the energy, kinetic and latent heat, goes to the bolometer. Equating the energies gives

$$E_b = E_h f_h f_g p_{pa} \tag{3}$$

and substituting the values above gives $p_{pa} = 2.3 \times 10^{-3}$.

To estimate the probability p_{ap}, we use data similar to that in figure 3 at 61.2°. To extract the sharp signal which is due to quantum condensation and starts at 92 μs, we interpolate the time-dispersed signal under it. The data with heater pulses of power 7.94 mW and duration 1 μs are used as this power gives the maximum value of the ratio of detected energy to input energy, see figure 10, and hence the maximum value of p_{ap}. At higher powers the surface of the liquid helium is spoiled by the higher atom flux and this gives lower values of p_{ap}. With the atom beam at 45° to the surface normal and the detector at 61.2°, the detected energy is $E_b = 2.25 \times 10^{-16}$ J for an input energy $E_h = 7.94 \times 10^{-9}$ J.

The collimator reduces the energy flux on the bolometer by the ratio of the solid angle which the second collimator subtends at the heater to 2π sr. This factor must be multiplied by 2 to take into account that atoms are evaporated with a cosine distribution which makes the atom flux in the forward direction twice as large as the average flux. Also it must be multiplied by 0.7 as this is the fraction of the 1 mm^2 heater area that contributes to the flux through the collimation. These geometrical effects give a total factor $h_g = 1.23 \times 10^{-3}$.

As we are considering phonons with energy $\epsilon_p > 10$ K then only atoms with energy $\epsilon_a > 3$ K contribute to the signal. For a helium film at 1.13 K, we calculate that a fraction $h_\epsilon = 0.51$ of the evaporating flux of atoms have energy >3 K.

The Zn bolometer detects the created high-energy phonons with a probability p_{pb}. The value of this probability can be estimated from the measurements of the phonon transmission into a solid [19, 20]. There are two channels for phonon transmission, the peak and background channels. The former is the classical acoustic channel and only applies over a narrow critical cone about the normal to the interface, on the liquid helium side. The transmission coefficient normal to the interface is $p_{pb}^{(pk)} \approx 4Z_H/Z_s$ where Z_H and Z_s are the acoustic impedances of the helium and solid respectively. $Z = \rho c$ where ρ is the density and c is the velocity of sound. In the solid the transmission is dominated by the transverse phonons so we use their velocity and find $p_{pb}^{(pk)} = 7.9 \times 10^{-3}$. The peak channel is independent of phonon frequency and the direction of the transmission through the interface.

In contrast the background channel applies at all angles of incidence on the helium side of the interface. This channel is due to localized imperfections in the surface, which breaks the translational invariance. The imperfections act as momentum reservoirs so the component of momentum parallel to the surface is no longer conserved and phonons at all angles of incidence have a probability of transmission through the interface. The transmission coefficient is dependent on phonon energy and rises linearly from zero at zero energy to a constant value at a phonon energy $\epsilon_p = 5$ K. It depends on the direction of transmission and is higher from solid to helium by a factor c_s^2/c_H^2 than from helium to solid; for ^{4}He and Zn this factor is 105. The saturation value from solid to helium has been found to be 0.5 [20]. Hence we find that the transmission probability from helium to zinc is

$$p_{pb}^{(bg)} = \begin{cases} 9.5 \times 10^{-4}\epsilon_p, & 0 < \epsilon_p < 5 \text{ K} \\ 4.8 \times 10^{-3}, & \epsilon_p > 5 \text{ K} \end{cases} \tag{4}$$

where ϵ_p is the phonon energy in kelvin.

As the Zn bolometer has a rough surface, the incident phonons mainly have angles of incidence, to the local surface, which are outside of the critical cone, so the background channel dominates the transmission. So we take $p_{pb} = 4.8 \times 10^{-3}$ in this analysis for phonons with $\epsilon_p > 10$ K. It is worth noting that this value is the same order of magnitude as $p_{pb}^{(pk)} = 7.9 \times 10^{-3}$, so the surface roughness is not such a crucial issue for the detection of high-energy phonons as it is for low-energy phonons. Equating energies we get

$$E_b = E_h h_g h_\epsilon p_{pb} p_{ap} \tag{5}$$

and substituting the values above we find $p_{ap} = 9.4 \times 10^{-3}$.

We see that p_{ap} is $\approx 4 p_{pa}$ from these estimates. However, many of the factors have uncertainties of $\overset{\times}{\div} 2$ so we do not rule out that $p_{ap} = p_{pa}$ as predicted under restrictive conditions by Dalfovo *et al* [28].

The value of p_{pa} is much smaller than our previous estimate [25]. Previously we thought that high-energy phonons were directly injected into the helium by the heater and so very little of the injected energy was in the form of phonons with $\epsilon_p > 10$ K. Now we know that high-energy phonons are created in the helium from low-energy phonons and this process is very efficient [18, 24], and furthermore these phonons are strongly peaked in the forward direction. At low heater powers they are in a cone of angle 4° [30, 31]. This means that the beam of high-energy phonons, in quantum evaporation experiments, is much higher than previously thought. Correspondingly the derived value of p_{pa} is much smaller.

The present value of p_{pa} is much smaller than theoretical estimates [32–36].

4.3. Atom to ripplons to phonons

We ascribe the time-dispersed signal, examples are shown in figure 3 at angles of $35° < \theta < 70°$, to condensing atoms creating many ripplons which then interact and create phonons in the liquid helium. Besides this signal being the most time-dispersed, its other characteristics are

(a) it starts ≈ 7 μs earlier than the roton signal (see figure 4),
(b) it is not strongly affected by the ambient temperature (see figure 7) and
(c) it peaks at an angle $\theta \approx 50°$ which is far from the roton angle and distinct from the angle for the one atom to one phonon process.

Its peak height is only ≈ 0.05 of that of the rotons but is comparable to that of the high-energy phonons. These characteristics clearly point to low-energy phonons which have a high velocity

in the liquid and are only weakly scattered by thermal phonons. We now consider how they are created.

One possibility might be that one atom creates two or more phonons in the liquid. This is a higher order process than one atom creating one phonon and so can be reasonably expected to have a lower probability. However, we see that the integrated energy in the time-dispersed signal is more than an order of magnitude greater than the single phonon signal. So we conclude that the origin of this signal is not the creation of two phonons.

Another possibility might be that an atom creates a phonon and a ripplon. This is another higher order process. Also one would expect the phonons to be created at all angles in the liquid. This is because the momentum of the ripplon can be similar to that of a low-energy phonon and can be in any direction. To conserve parallel components of momentum, the phonon and ripplon must have corresponding directions. The parallel momentum of the ripplon can be in any direction, so the direction of the phonon is decoupled from the direction of the incident atom. As we find these phonons are confined to angles $\theta = 50 \pm 15°$, we rule out this process.

What we believe is happening is that condensing atoms readily create ripplons and a large ripplon population builds up on the surface of the liquid helium. The ripplons strongly interact with each other and rapidly come into thermal equilibrium on a timescale $\approx 10^{-6}$ s at $T = 0.2$ K [37]. They form a moving group because the integrated parallel component of momentum of the atoms is given to the ripplon system as a whole. On a slower timescale, there are ripplon–ripplon interactions that create low-energy phonons, $\mathrm{r}_1 + \mathrm{r}_2 \rightarrow \mathrm{l}_3$ [37]. The created phonons are centred about a direction which again preserves the parallel component of momentum in the created phonon system.

We can estimate the temperature of the ripplons from the flux of energy delivered by the condensing atoms and the decay rate of the ripplon system. The ripplon density can decay in two ways: by the creation of phonons, and by ripplons propagating away from the area where they were created. As this area has dimensions of order 1 mm^2 and a ripplon with energy 0.2 K has a velocity 60 m s^{-1} then the characteristic timescale is of order $10^{-3}/60 = 1.6 \times 10^{-5}$ s. The time will be longer due to ripplon interactions. This time is larger than the inverse of the phonon creation rate for ripplons of the same energy, so we only consider loss due to phonon creation.

From Reynolds' results [37] we find that the decay rate to the production of phonons can be expressed as

$$\Gamma_3 = \frac{4\hbar\omega^3 p^2}{3\pi\rho c^3} n(\omega) \tag{6}$$

where $\hbar\omega$ and $\hbar p$ are the energy and momentum of the ripplon respectively, $n(\omega) = [\exp(\hbar\omega/k_B T) - 1]^{-1}$, ρ is the density of ^{4}He and c is the velocity of sound in ^{4}He. We have dropped the term $-n(2\omega)$ in equation (65) in [37] as there are no phonons in the cold liquid ^{4}He to create ripplons.

The rate of energy loss of ripplons is equal to the rate of energy gain by the created phonons, $\dot{E}_p$, and is given by

$$\dot{E}_p = \int_0^\infty 2\Gamma_3 \hbar\omega N(\omega) n(\omega)\, \mathrm{d}\omega \tag{7}$$

where $N(\omega)$ is the density of ripplon states given by

$$N(\omega) = \frac{A\omega^{1/3}}{3\pi\alpha^{4/3}} \tag{8}$$

where A is the area of ^{4}He surface. The factor 2 in equation (6) is because two ripplons are lost on each scattering. We assume that $\omega = \alpha p^{3/2}$ where p is the wavevector of the ripplon

and $\alpha = (\sigma/\rho)^{1/2} = 1.546 \times 10^{-3}$ J$^{1/2}$ m$^{1/2}$ kg$^{-1/2}$ using the value of the surface tension $\sigma = 3.546 \times 10^{-4}$ J m^{-2} [38] and $\rho = 145$ kg m^{-3}. Evaluating this integral we find

$$\dot{E}_p = \frac{8Ak_B^{20/3}}{9\pi^2\alpha^{8/3}\rho c^3\hbar^{14/3}} T_r^{20/3} \int_0^\infty \frac{x^{17/3}}{(e^x - 1)^2}\,dx \tag{9}$$

where T_r is the ripplon temperature. The integral $= 4.51$.

We measured the atom flux from the heater in the same experimental run when the liquid level was below the bolometer. We found that the time dependence of the atom flux in the normal direction is consistent with the evaporation from heated liquid helium at temperature T. The number of atoms with wavevectors between k and $k + dk$ that leave the helium surface between θ and $\theta + d\theta$ and between ϕ and $\phi + d\phi$ is

$$\frac{\hbar k^3\,dk}{8\pi^3 m} \exp\left(-\frac{\hbar^2k^2}{2mk_BT}\right) \exp\left(-\frac{L}{k_BT}\right) \sin\theta\cos\phi\,d\theta\,d\phi\,\delta A_h\tau_p \tag{10}$$

where L is the latent heat per atom, m is the mass of a ^{4}He atom, δA_h is the area of the heated liquid helium film and τ_p is the length of time of the short heater pulse. With a pulse power of 0.5 mW we find that the atom signal as a function of time gives a heater temperature $T_h = 0.8$ K. From equation (9) and $\hbar k = ml/t$ where l is the path length of the atom beam, we calculate the number of atoms that arrive between t and $t + dt$ on the surface of the liquid as

$$\frac{\hbar^2k^5\,dt}{8\pi^3 ml} \exp\left(-\frac{\hbar^2k^2}{2mk_BT}\right) \exp\left(-\frac{L}{k_BT}\right) \sin\theta\cos\phi\,d\theta\,d\phi\,\delta A_h\tau_p. \tag{11}$$

The energy flux, $\dot{E}_a$ delivered on a small area δA_l of the surface whose normal is at an angle θ to the beam at time t, where $t \gg \tau_p$, is then given by

$$\dot{E}_a = \frac{\cos\theta m^3 l^2 \delta A_h \delta A_l \tau_p}{8\pi^3\hbar^3 t^5} \left(\frac{ml^2}{2t^2} + k_BL\right) \exp\left(\frac{-ml^2}{2t^2k_BT}\right) \exp\left(\frac{-L}{k_BT}\right) \tag{12}$$

for an atom beam perpendicular to the heater.

The atoms arriving at the surface of the liquid increase the ripplon temperature, T_r, and the ripplons create phonons which propagate away from the surface. From the conservation of energy and putting $A = \delta A_l$. we find

$$\int_0^t \dot{E}_a\,dt = \int_{T_i}^{T_r(t)} C(T_r)\delta A_l\,dT_r + \int_0^t \dot{E}_p\,dt \tag{13}$$

where $C(T_r)$ is the heat capacity of the ripplons per unit area which is given by

$$C(T_r) = \frac{7k^{7/3}T_r^{4/3}}{9\pi\alpha^{4/3}\hbar^{4/3}} \int_0^\infty \frac{x^{4/3}\,dx}{e^x - 1}. \tag{14}$$

The value of the integral is 1.685. The solution of the rate equation is shown in figure 8. The curve labelled 'flux-in' is the energy flux $\dot{E}_a$ on the helium surface arising from the condensing atoms when the heater temperature is 1.13 K for 2 μs. Because a spectrum of atoms is created, the flux at the liquid surface is dispersed over $\approx$30 μs. The curve labelled 'flux-out' is the energy flux carried away by the created phonons, $\dot{E}_p$. We see that the phonon energy flux follows the atom energy flux in amplitude and with only a small time lag of $\approx$3 μs at the start. This is due to the relatively small energy required to create the ripplon population. This energy is essentially supplied in the first few microseconds of the atom flux. In figure 8, the ripplon temperature is shown as a function of time. We see that the ripplon temperature rises in $\approx$10 μs to $T_r = 0.27$ K. It decays on a very long timescale due to phonon emission. This long time follows from the strong temperature dependence of the phonon emission rate,

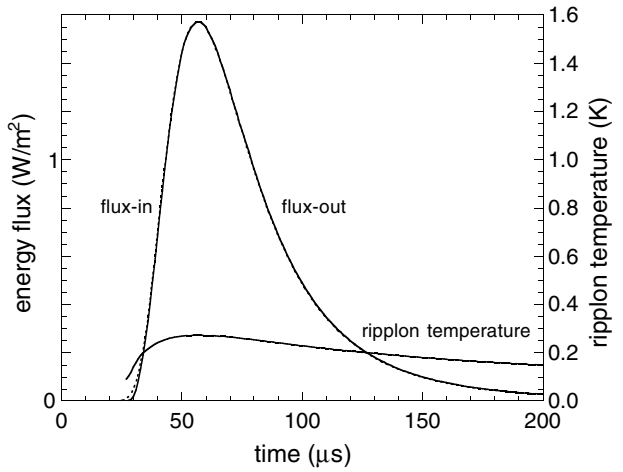

Figure 8. Calculated energy flux on the liquid helium surface due to the atom beam: 'flux-in' (dotted curve), the calculated energy flux from the surface carried away by the created phonons, 'flux-out' (solid curve) and the temperature of the ripplons as a function of time. The heater pulse is 8 mW and 2 μs giving $T_h = 1.13$ K.

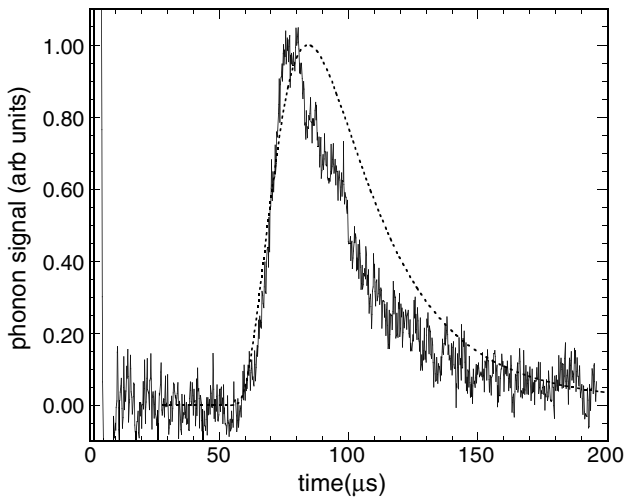

Figure 9. Calculated energy flux on the bolometer due to phonons created from ripplons and the measured signal with $\phi = 45°$ and $\theta = 45°$; the heater pulse is 8 mW and 2 μs giving $T_h = 1.13$ K. The curves are normalized at the peaks.

$T_r^{20/3}$, in equation (5). For example, when T_r drops from 0.20 to 0.15 K, the phonon creation rate drops by a factor of 6.

In figure 9 we compare the phonon energy flux from ripplons to the measured signal at $\theta = 45.4°$. We see that the fit is good for the leading edge, which gives us confidence in the ripplon picture. However, the signal decays faster than that calculated which we suspect is due to ripplons escaping from the small area where they are produced. The time difference is consistent with our estimate of the ripplon escape time made earlier.

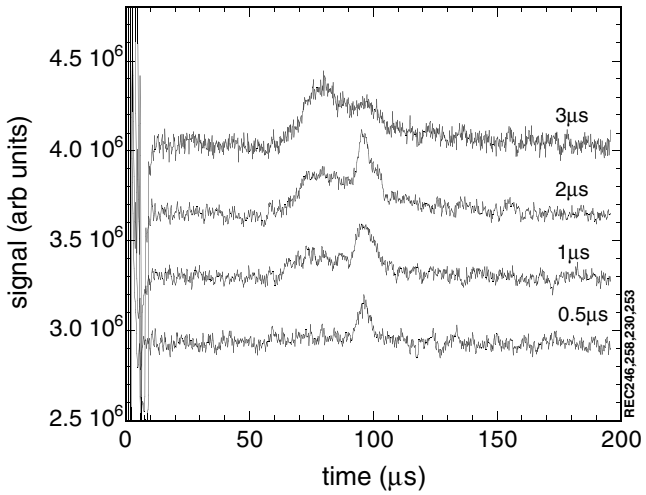

Figure 10. Signals of the low- and high-energy phonons as a function of heater pulse length $\phi = 45°$ and $\theta = 62°$; the heater pulse is 8 mW. The high-energy phonons disappear at 3 μs due to surface spoiling at high atom fluxes. The same vertical scale is used for all the curves which are offset vertically.

4.4. Heater power and pulse length dependence

The quantum condensation phonon signal and the multi-phonon signal from ripplons behave differently as a function of heater power and pulse length. This is clearly shown by the signals in figure 10 where the high-energy phonon signal has almost disappeared when the pulse length has increased to 3 μs. Figures 11 and 12 show that the time-integrated low-energy phonon signals increase linearly with heater power and pulse length. Such behaviour follows if the energy in the ripplons is directly proportional to the energy of the atoms that condense from one pulse. For this, the length of the atom pulse on the liquid surface must be short on the timescale of the ripplon loss rate to other than phonons. When the pulse length is long compared to this time then we would expect a proportionality constant that is smaller and depends on the branching ratio of the two losses, to phonons and to other than phonons, which will be a function of the temperature of the ripplons.

In contrast, the quantum condensation phonon signal shows a maximum as a function of both heater power and pulse length. We attribute this to the free surface of the liquid helium being spoiled when the flux of atoms is too large. The one atom to one phonon signal is concentrated into angles around $\theta = 60°$ by the conservation laws expressed in equations (1) and (2). For equation (2) it is assumed that the surface has translational invariance. If it does not but the surface height changes gradually, the equations apply locally and the created phonons are angularly dispersed so weakening their flux around these angles. However, when the surface is rough, on the scale of $\approx 10 \times k_{\parallel}^{-1}$, then the equations become even less applicable. We would expect the spoiling to increase with the ripplon density and hence with the atom flux.

So we can now qualitatively understand the behaviour of the quantum condensation phonon signal. At low atom fluxes, the signal initially increases linearly but, as the atom flux is increased, the spoiling of the surface is increased and the sharp phonon signal ceases to increase and eventually drops to zero. This happens when the created phonons are spread over such a large solid angle that their signal disappears into the noise.

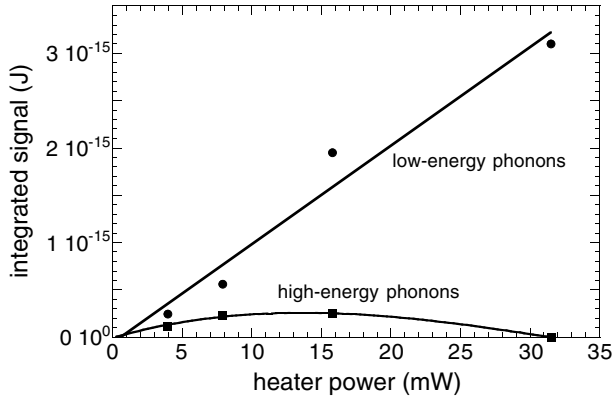

Figure 11. Signals integrated over time, for the low-energy phonons from ripplons and the high-energy phonons as a function of heater pulse power. $\phi = 45°$ and $\theta = 62°$; the heater pulse is 1 μs.

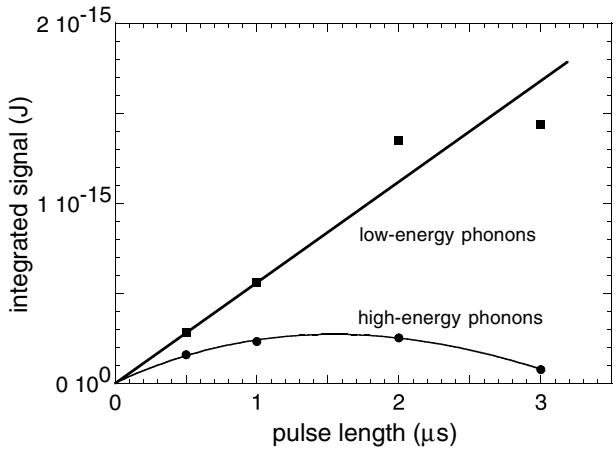

Figure 12. Signals integrated over time, for the low-energy phonons from ripplons and the high-energy phonons as a function of heater pulse length. $\phi = 45°$, $\theta = 62°$ and the heater pulse is 8 mW.

5. The creation of R^+ rotons

5.1. Signal at the R^+ roton angle

By far the largest signal in figure 4 is at the angle for one atom to one R^+ roton processes. Although we shall conclude that this is evidence for this quantum condensation process, the attribution is not completely straightforward. The first, and most significant, question concerns what we are detecting at this roton angle. Over the course of very many experiments on propagating excitations through liquid ^{4}He to a bolometer in the liquid, we have never seen a signal which we can attribute to rotons. We can, however, detect R^+ rotons by quantum evaporation and we can find the best heater conditions for producing ballistic R^+ rotons, which are low power and long pulses, typically 2 mW and 10 μs. So we know that we can arrange for a bolometer in the liquid to be in an R^+ roton flux, albeit with an accompanying low-energy phonon flux.

In quantum evaporation we can measure the time of flight for the combined R^+ roton and atom path, and also the angle of refraction expressed in equation (2). Both these measurements show that a wide spectrum of R^+ rotons is created by the heater and can propagate, without decay, over distances of order 10 mm to the surface of the liquid [4, 39]. The time of flight of 71 μs for 6.5 mm in the liquid and 6.6 mm in the vacuum shows that R^+ rotons of energy $\epsilon_{R+} =$ 12.5 K are present. At the other end of the roton energy scale, scattering experiments [43, 44] show that R^+ rotons with energy $\epsilon_{R+} \approx 10$ K ($q = 2.1$ Å^{-1}, $v_g = 166$ m s^{-1}) are also created. The angular distribution of atoms from R^+ rotons at an angle of incidence of 14° is consistent with a number density of rotons proportional to q^2 /[exp($\epsilon_{R+}/k_B T_{R+}$) − 1] with T_{R+} between 1 and 1.5 K [4, 15, 45]. So the evidence is that a wide spectrum of R^+ rotons is created by a heater and, most importantly for interpreting the condensation results, can propagate without decay over many millimetres. The number of R^+ rotons with energy >2.5 K is small, due to the exponential decrease with energy, and so their presence is increasingly difficult to detect.

When we try and detect these heater-generated R^+ rotons in the liquid ^{4}He with a detector, usually a Zn bolometer, we see *only* a large low-energy phonon signal. This travels at 238 m s^{-1} and so lasts for essentially the time of the heater pulse as the bolometer relaxation time is short, <1 μs. The R^+ roton flux is dispersed with group velocities between 0 and ≈ 238 m s^{-1}. The very slow R^+ rotons are most dispersed and so will have a very low flux from a pulsed source. Hence their signal disappears into the noise. However, rotons with velocity somewhat slower than 238 m s^{-1} should be well separated in time from the low-energy phonons and have a relatively large flux. Indeed, such rotons have been seen in roton–roton scattering experiments where quantum evaporation was used to detect them [43, 44].

There are two possible reasons why the R^+ rotons are not detected by a bolometer in the liquid ^{4}He. The first is that the number of rotons created by the heater is so much smaller than the number of phonons that it is difficult to see a small and featureless signal just as the bolometer and the electronics are recovering from the large phonon signal. This recovery involves higher order poles in the frequency response and so the last stage of the recovery is not a simple exponential decay with one time constant. The second possibility is that R^+ rotons do not easily create phonons in the bolometer, which is the first stage of the detection process, prior to the energy going into the electron system. It is indeed likely that rotons have a high probability of reflection from the solid surface of the detector, with a mode change and with little energy or momentum exchange with the solid. We consider these possibilities in the next section.

Returning to the condensation signal at the R^+ roton angle, we conclude that as rotons created at the surface can propagate without decay to the bolometer, the signal is due to the rotons being directly detected by the bolometer. We are seeing them, in this case, because they are the dominant excitation flux on the bolometer. The roton flux from condensation is much larger than from a heater because of the much higher probability of atoms creating rotons (≈0.4). This higher flux compensates for their weak interaction with the bolometer.

In figure 13 we show typical atom to R^+ roton signals at various bath temperatures. The fastest part of the signal at 83 mK arrives at 71 μs which corresponds to an atom with energy 5.3 K and an R^+ roton with energy 12.46 K. As the temperature is raised the roton flux is attenuated by the rotons scattering with the thermal phonons. The behaviour is similar to that found by quantum evaporation [27] where it is found that theory [46] gives a good description of the behaviour. The front of the signal is attenuated first, as the temperature is increased, so it is clear that the faster, higher energy R^+ rotons are much more strongly attenuated than the slower, lower energy ones.

The R^+ roton signal at the lowest temperatures increases linearly with the heater power as shown in figure 14, although this will not continue indefinitely. In figure 15 we show the roton

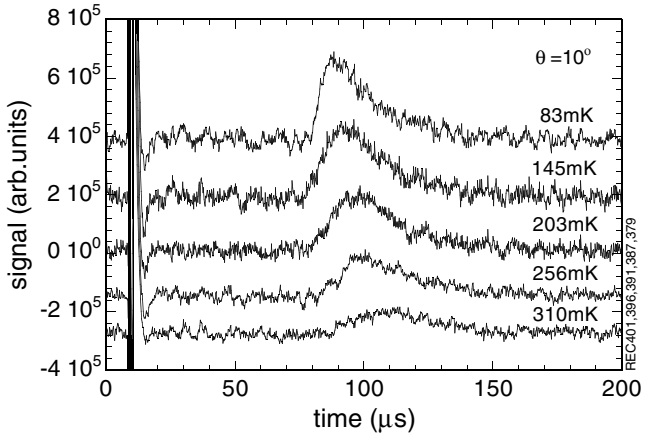

Figure 13. The one atom to one R^+ roton signal as a function of bath temperature. $\phi = 45°$ and $\theta = 10°$, the heater pulse is 1 mW and 2 μs.

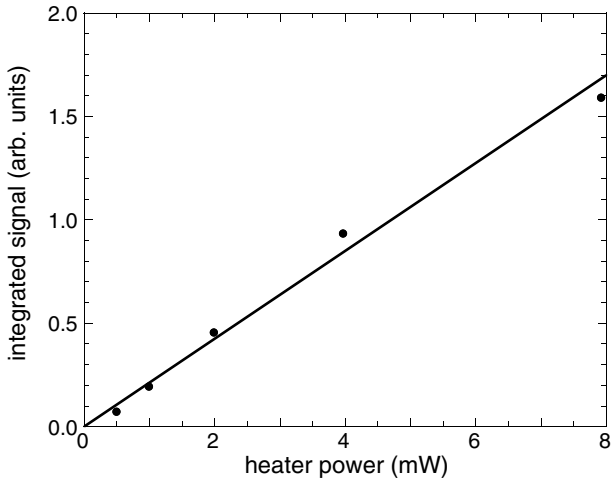

Figure 14. The one atom to one R^+ roton signal, integrated over time, as a function of heater power. $\phi = 45°$, $\theta = 15°$ and the heater pulse is 2 μs.

signal as a function of angle at various heater powers. The angular width increases slightly with heater power in this range. However, at higher powers the width increases substantially [6] due to surface spoiling.

5.2. Creation and detection probabilities

To show that there is a consistent picture in evaporation and condensation, we must consider the probabilities of heaters and atoms creating rotons and the sensitivity of the bolometer in detecting rotons and atoms.

We first consider a heater immersed in liquid ^{4}He and estimate the fraction of electrical energy that goes to creating R^+ rotons. Relatively long and low power pulses (10 μs, 2 mW mm^{-2}) are best for creating ballistic R^+ rotons. This compares to the short and

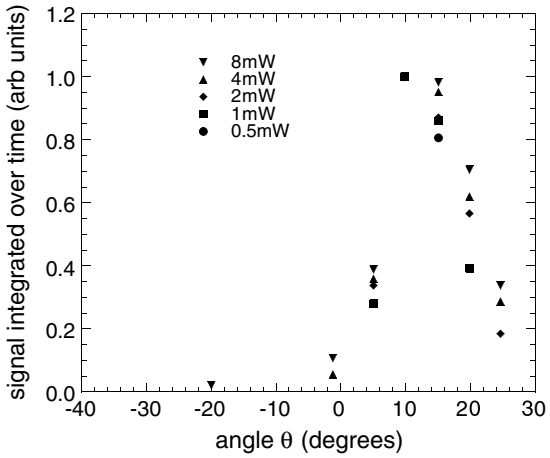

Figure 15. The one atom to one R^+ roton signal, integrated over time, as a function of angle for various heater powers. $\phi = 45°$ and the heater pulse is 2 μs. The results are normalized at 10°.

higher power (100 ns, 20 mW mm^{-2}) pulses that are necessary to create high-energy phonons ($\epsilon_p > \epsilon_c = 10$ K) from low energy phonons. In both cases many low-energy phonons are created by the heater.

Rotons are most readily detected by quantum evaporation. In fact, the results presented in this paper are the first clear evidence that rotons can be detected by a bolometer in the liquid. To measure the quantum evaporation signal we rotated the heater and the collimator, used in the condensation experiment, to be in the liquid in order to create a beam of rotons directed at the free surface of the liquid, in the perpendicular direction. The atoms, quantum evaporated by the rotons, are detected by a bolometer which is set at several angles, ϕ, about the normal in the vacuum above the liquid. First the energy in the atom signal is integrated over time, which we define as $F(\phi)$, and, second, over angle to give the energy $E_a^{(QE)}$ using the relation

$$E_a^{(QE)} = \frac{2\pi R^2}{A} \int_0^{\phi_{max}} F(\phi) \sin(\phi)\, \mathrm{d}\phi \tag{15}$$

where $R = 6.6$ mm is the distance from the bolometer to the surface of the liquid along the axis defined by the collimator; $F(\phi)$ is the energy that goes into the area, A, of the bolometer. We asume that this is the area of the superconducting track: 1 mm^2 in these experiments. If the bolometer is not uniformly sensitive, then the value of $E_a^{(QE)}$ will be greater. After numerically integrating equation (14) we find the energy in the atoms is $E_a^{(QE)} = 4.1 \times 10^{-13}$ J for 2 mW and 10 μs heater pulses.

The energy in the heater pulse is $E_h = 2 \times 10^{-8}$ J. Let p_{h+} be the fraction of the heater energy that gets converted to R^+ rotons, g be the fraction of the rotons that get through the collimation and p_{+a} be the probability that one R^+ roton evaporates one atom. We assume that the rotons are created with a cosine distribution so that the flux in the direction normal to the heater is twice the average flux. Then $g = 2\Omega_{col}/2\pi$, where Ω_{col} is the solid angle subtended by the collimator aperture nearest the heater. For the aperture 0.4 mm $\times$ 1 mm, at a distance 4.5 mm from the heater, $\Omega_{col} = 1.98 \times 10^{-2}$ and hence $g = 6.29 \times 10^{-3}$.

We next assume that $p_{+a} = 0.35$, which is consistent with the transmission experiment [47] and other estimates [40, 41]. By equating energies we find the following equation for p_{h+}:

$$p_{h+} = \frac{E_a^{(QE)}}{E_h g p_{+a}} \tag{16}$$

and substituting the values given above into equation 12 we obtain $p_{h+} = 9.3 \times 10^{-3}$. In [42] we found that 0.5% of the heater energy went to creating large-wavevector R^+ rotons, on the basis that the probability of quantum evaporation is one and that the R^+ rotons are emitted isotropically. If we use the present assumptions of $p_{+a} = 0.35$ and a cosine distribution then $p_{h+} = 7.7 \times 10^{-3}$, which is essentially the same as we find here. So we see that under optimized pulse conditions only ≈1% of the heater energy goes to R^+ rotons, the remainder going to low-energy phonons. The density of these phonons is too low for them to create a significant number of high-energy phonons.

We now turn to the condensation results and do a similar analysis. We take the measured data, similar to those in figure 3, and integrate over time and angle to find the total detected energy in the R^+ roton signal is $E_+^{(C)} = 5.1 \times 10^{-14}$ J for a heater pulse of $W = 8$ mW and $t_p = 2$ μs. We assume that all the heat goes into evaporating atoms. The fraction of atoms that gets through the first collimator is again $g = \Omega_{col}/\pi$ as the atoms from a heater have a cosine distribution. From the slowest arriving R^+ roton signal we calculate that only atoms with $\epsilon_a > 3$ K create detectable R^+ rotons. Assuming that the heater temperature is governed by the evaporation heat loss, we calculate that the heater temperature is 1.13 K for 8 mW heater pulses. For this temperature the fraction, h_ϵ, of atoms evaporated with energy >3 K we calculate to be 0.51. So the energy, $E_a^{(C)}$, which includes the 7.16 K potential energy, in the atoms that get through the collimator and condense on the liquid surface is given by

$$E_a^{(C)} = W t_p g h_\epsilon \tag{17}$$

giving $E_a^{(C)} = 5.13 \times 10^{-11}$. If we call the probability of an atom creating a R^+ roton p_{a+} and the fraction of the R^+ roton energy that goes into the bolometer p_{+b}, then the total energy in the R^+ roton signal $E_+^{(C)}$, integrated over time and angle, is given by

$$E_+^{(C)} = E_a^{(C)} p_{a+} p_{+b}. \tag{18}$$

Using this equation and taking $p_{a+} = 0.35$ we find $p_{+b} = 2.8 \times 10^{-3}$.

We are now in the position to see why we do not detect rotons when both the heater and bolometer are in the liquid. A low-power heater pulse (around 2 mW mm^{-2}) creates both low-energy phonons and R^+ rotons. The low-density, low-energy phonons decay as they propagate and reach a phonon energy $\epsilon_p \approx 0.5$ K by the time they reach the bolometer. From equation (4) we see that $p_{pb} = p_{pb}^{(bg)} = 4.8 \times 10^{-4}$ for these phonons detected by a rough bolometer, where essentially all the detection is via the background channel. As a check, this value of p_{pb} gives the correct magnitude for the phonon signal, from long low-energy pulses (5 mW, 5 μs), directly detected in the liquid helium. We see that p_{pb} is an order of magnitude smaller than $p_{+b} = 2.7 \times 10^{-3}$.

The ratio of the time-integrated energies, in the bolometer, of the R^+ roton and phonon signals is given by the ratio of the creation probabilities multiplied by the ratio of the transmission probabilities into the bolometer, i.e.

$$\frac{E_+}{E_p} = \frac{p_{h+}}{(1 - p_{h+})} \frac{p_{+b}}{p_{pb}} \tag{19}$$

and substituting $p_{h+} = 9.3 \times 10^{-3}$, $p_{+b} = 2.8 \times 10^{-3}$, $p_{pb} = 4.8 \times 10^{-4}$, the phonon transmission for a rough bolometer, we find $E_+/E_p = 5.6 \times 10^{-2}$. We see that the energy in the R^+ roton bolometer signal is more than an order of magnitude smaller than that in the low-energy phonon bolometer signal. As the R^+ roton signal is dispersed in time but the phonon signal is not, the peak R^+ roton signal will be more than two orders of magnitude lower than the peak phonon signal. This means that the roton signal is just too small to be detected in this situation. However, we can detect the same flux of rotons by quantum evaporation because

R^+ rotons evaporate atoms with high probability ($\approx$0.35) and all the atoms are detected by the bolometer as they condense on the ^{4}He film covering the bolometer with essentially unit probability.

In the condensation experiment we can directly detect the R^+ roton beam because the roton beam is much more intense than from a heater immersed in the liquid. The reason for this is that atoms create rotons with a high probability, $\approx$0.4, while a heater creates them with a low probability, $\approx 9.3 \times 10^{-3}$. They are also not obscured by low-energy phonons.

6. Conclusions

Our experiments on the condensation of a beam of ^{4}He atoms onto cold liquid ^{4}He show that both phonons and R^+ rotons are created in one-to-one processes. We detect these quantum condensed phonons if they have energy $\epsilon_p > 10$ K, as these phonons do not decay and so remain in a small solid angle with a measurable flux. There is no reason to suppose that low-energy phonons, $\epsilon_p < 10$ K, are not also created by quantum condensation. However, these phonons decay and are then spread over a larger solid angle, which makes them impossible to detect. The probability that a condensing atom will create a phonon with $\epsilon_p > 10$ K is low. We estimate $p_{ap} = 9.4 \times 10^{-3}$.

Condensing atoms have a much higher probability of creating R^+ rotons. Transmission measurements through a slab of liquid ^{4}He give the average value of the product of the condensation and evaporation probability as $p_{a+}p_{+a} = 0.12$ [47]. If we assume $p_{a+} = p_{+a}$ then $p_{a+} = 0.35$. Corresponding to this high value, a large flux of R^+ rotons is incident on the bolometer and so R^+ rotons can be directly detected. This is the first clear evidence for the direct detection of R^+ rotons, although they can be detected by quantum evaporation. From our results, we estimate that the probability of an R^+ roton giving its energy to the bolometer is $p_{+b} = 2.8 \times 10^{-3}$. This is similar to that for a high-energy phonon and an order of magnitude larger than that for a low-energy phonon ($\epsilon_p = 0.5$ K) detected by a rough bolometer where the background channel dominates.

We show that directly detecting R^+ rotons from a heater with the bolometer in the liquid is very difficult as the signal from the low-energy phonons obscures the potential signal from the R^+ rotons. We estimate that a heater using long and low-power pulses to optimize the production of R^+ rotons only gives $p_{h+} = 9.3 \times 10^{-3}$ of its energy to the R^+ rotons and the balance goes to producing low-energy phonons. It is clear that condensing atoms can create a much higher flux of R^+ rotons than a heater in liquid ^{4}He.

We find there is no detectable signal due to R^- rotons. This is not unexpected as the quantum evaporation probability p_{-a} is two orders of magnitude lower than that for R^+ rotons [3]. A signal 1/300 of the R^+ roton signal would not have been detectable.

Our experiments show that ripplons are the most likely excitations to be produced by condensing atoms. The probability of ripplon creation is $p_{ar} = (1 - p_{a+} - p_{ap}) \approx 0.65$. The ripplon population rapidly increases in the initial stages of the atom pulse because the heat capacity of the ripplons is very low. The ripplon density comes into a dynamic equilibrium, with the decay rate to phonons balancing the creation rate due to condensing atoms. We derive the rate equations and use Reynolds' expression, [37], for the ripplon lifetime due to the creation of phonons. We find that the ripplon temperature rises to $T_r = 0.27$ K. The energy in the created phonons has essentially the same time dependence as the energy released by the condensing atoms because of the low heat capacity of the ripplons. Indeed, we find that the phonon signal calculated on this basis agrees reasonably well with the measured signal as shown in figure 9.

The ripplons created by condensing atoms are an interesting system as they constitute a hot surface on otherwise cold liquid ^{4}He. They are in thermal equilibrium because of their

Table 1. Table of probabilities.

$p_{h+} = 9.3 \times 10^{-3}$	Heater creating R^+ rotons with $\epsilon_+ > 10$ K
$p_{hp_l} = 0.98$	Heater creating low-energy phonons, $p_{hp_l} = 1 - p_{h+} - p_{hp_h}$
$p_{hp_h} \approx 1 \times 10^{-2}$	Heater creating high-energy phonons; depends on the heater temperature
$p_{+b} = 2.8 \times 10^{-3}$	Rotons giving energy to the bolometer
$p_{pb}^{pk} = 7.9 \times 10^{-3}$	Phonons giving energy to the bolometer via the peak channel; independent of phonon frequency
$p_{pb}^{bg} = 9.5 \times 10^{-4}\epsilon_p$	$\epsilon_p < 5$ K; phonons giving energy to the bolometer via the background channel
$= 4.8 \times 10^{-3}$	$\epsilon_p > 5$ K
$p_{sH} = 0.1\epsilon_p$	$\epsilon_p < 5$ K; transmission from solid Zn to liquid helium and averaged over phonons in the solid Zn
$= 0.5$	$\epsilon_p > 5$ K
$p_{pa} \approx 2.2 \times 10^{-3}$	Phonon quantum evaporation
$p_{ap} \approx 9.4 \times 10^{-3}$	Phonon quantum condensation
$p_{+a} = 0.35$	R^+ roton quantum evaporation [40]
$p_{a+} = 0.34$	R^+ roton quantum condensation, from average $p_{a+}p_{+a} = 0.12$ [47] and $p_{+a} = 0.35$
$p_{ar} = 0.65$	Atom creating ripplons, from $p_{ar} = (1 - p_{a+} - p_{ap})$
$p_{-a} = p(\epsilon_-)$	$p(\epsilon_-) = 2.3 \times 10^{-4} \exp[0.9(\epsilon_- - 8.6)]$ [16]

rapid three-ripplon scattering, [37], and the population can decay by ripplon escape and by creating phonons. The present work shows that ripplons can be investigated by detecting these created phonons.

We have analysed the size of the various signals that we have detected, in terms of the input energy and the sequence of probabilities involving getting through the collimation, creation processes at the liquid helium surface and detection probabilities. As many of these estimated values are new, we summarise them in table 1.

We derived a value for the probability p_{pa}, for a phonon with $\epsilon_p = 10$ K to quantum-evaporate one atom. The value of $p_{pa} = 2.2 \times 10^{-3}$ is a quarter of that of $p_{ap} = 9.4 \times 10^{-3}$. Because of the uncertainties in the various estimates (we are accounting for a difference of over six orders of magnitude between input and detected energies) we cannot say that $p_{pa} \neq p_{ap}$. For R^+ rotons and atoms the values of p_{+a} and p_{a+} are much closer. If we take $p_{+a} = 0.35$ [40] and the average value of $p_{+a}p_{a+} = 0.12$ [47] we see that $p_{a+} = 0.34$. In [28] it is argued, from unitarity and time reversal symmetry applied to just atoms, phonons, R^- rotons and R^+ rotons in one-to-one processes, that $p_{ea} = p_{ae}$, where e is an excitation in the bulk ^{4}He. The above values show that this may well be true for R^+ rotons.

Just as quantum evaporation has enabled the study of ballistic high-energy phonons and rotons, so too quantum condensation promises to further the study of roton–roton interactions. The high flux of R^+ rotons produced by condensation will enable new scattering experiments to be done.

The most important conclusion from these experiments is that condensing helium atoms can produce phonons and R^+ rotons in one-to-one processes. Quantum condensation, the time reverse of quantum evaporation, exists.

Acknowledgments

It is a pleasure to acknowledge discussions with C D H Williams, L Pitaevskii and I N Adamenko, and grants from EPSRC.

References

[1] Baird M J, Hope F R and Wyatt A F G 1983 *Nature* **304** 325
[2] Hope F R, Baird M J and Wyatt A F G 1984 *Phys. Rev. Lett.* **52** 1528
[3] Tucker M A H and Wyatt A F G 1999 *Science* **283** 1150
[4] Brown M and Wyatt A F G 1990 *J. Phys.: Condens. Matter* **2** 5025
[5] Edwards D O, Ihas G G and Tam C P 1977 *Phys. Rev.* B **16** 3122
[6] Brown M and Wyatt A F G 1990 *Phonons 89* ed S Hunklinger, W Ludwig and G Weiss (Singapore: World Scientific) p 1050
[7] Cregan R F, Tucker M A H and Wyatt A F G 1995 *J. Low Temp. Phys.* **101** 531
[8] Nayak V U, Edwards D O and Mashura N 1983 *Phys. Rev. Lett.* **50** 990
[9] Edwards D O and Fatouros P P 1978 *Phys. Rev.* B **17** 2147
[10] Swanson D R and Edwards D O 1988 *Phys. Rev.* B **37** 1539
[11] Wyatt A F G, Tucker M A H and Cregan R F 1995 *Rev. Lett.* **74** 5236
[12] Sherlock R A and Wyatt A F G 1983 *J. Phys. E: Sci. Instrum.* **16** 673
[13] Sherlock R A 1984 *J. Phys. E: Sci. Instrum.* **17** 386
[14] Williams C D H 1990 *Meas. Sci. Technol.* **1** 322
[15] Williams C D H 1998 *J. Low Temp. Phys.* **113** 11
[16] Tucker M A H and Wyatt A F G 2000 *J. Low Temp. Phys.* **121** 333
[17] Havlin S and Luban M 1972 *Phys. Lett.* A **42** 133
[18] Wyatt A F G, Tucker M A H, Adamenko I N, Nemchenko K E and Zkukov A V 2000 *Phys. Rev.* B **62** 9402
[19] Wyatt A F G and Page G J 1978 *J. Phys. C: Solid State Phys.* **11** 4927
[20] Bradshaw T W and Wyatt A F G 1983 *J. Phys. C: Solid State Phys.* **16** 651
[21] Jackle J and Kerr K W 1971 *Phys. Rev. Lett.* **27** 654
[22] Dynes R C and Narayanamurti V 1974 *Phys. Rev. Lett.* **33** 1195
[23] Wyatt A F G, Lockerbie N A and Sherlock R A 1974 *Phys. Rev. Lett.* **33** 1425
[24] Adamenko I N, Nemchenko K E, Zhukov A V, Tucker M A H and Wyatt A F G 1999 *Phys. Rev. Lett.* **82** 1482
[25] Tucker M A H and Wyatt A F G 1996 *Czech. J. Phys.* **46** 263
[26] Tucker M A H and Wyatt A F G 1992 *J. Phys.: Condens. Matter* **4** 7745
[27] Tucker M A H and Wyatt A F G 1998 *J. Low Temp. Phys.* **110** 425
[28] Dalfovo F, Pitaevskii L and Stringari S 1996 *Czech. J. Phys.* **46** 391 see also [32]
[29] Tucker M A H, unpublished
[30] Tucker M A H and Wyatt A F G 1994 *J. Phys.: Condens. Matter* **6** 2825
[31] Vovk R, Williams C D H and Wyatt A F G, unpublished
[32] Dalfovo F, Fracchetti A, Lastri A, Pitaevskii L and Stringari S 1995 *Phys. Rev. Lett.* **75** 2510
[33] Guilleumas M, Dalfovo F, Oberosler I, Pitaevskii L and Stringari S 1998 *J. Low Temp. Phys.* **110** 449
[34] Sobnack M B, Matthias J R, Fung J C H, Williams C D H and Inkson J C 2002 *Phys. Rev.* B **65** 184521
[35] Campbell C E, Krotscheck E and Saarela M 1998 *Phys. Rev. Lett.* **80** 2169
[36] Krotscheck E, Apaja V and Rimnac A *Proc. LT23*
[37] Reynolds M W 1997 *J. Low Temp. Phys.* **108** 217
[38] Iino M, Suzuki M and Ikushima A J 1985 *J. Low Temp. Phys.* **61** 155
[39] Brown M and Wyatt A F G 1990 *Phonons 89* ed S Hunklinger, W Ludwig and G Weiss (Singapore: World Scientific) p 1053
[40] Fozooni P, Spencer D S and Lea M J 1987 *Japan. J. Appl. Phys.* **26 S26-3** 281
[41] Enss C, Bandler S R, Lanou R E, Maris H J, Moore T, Porter F S and Seidel G M 1994 *Physica* B **194** 515
[42] Brown M and Wyatt A F G 1990 *Phonons 89* ed S Hunklinger, W Ludwig and G Weiss (Singapore: World Scientific) p 1056
[43] Forbes A C and Wyatt A F G 1990 *Phys. Rev. Lett.* **64** 1393
[44] Wyatt A F G and Forbes A C 1990 *Excitations in Two-Dimensional and Three-Dimensional Quantum Fluids* ed A F G Wyatt and H Lauter (New York: Plenum) p 137
[45] Williams C D H 1998 *J. Low Temp. Phys.* **113** 627
[46] Landau L D 1949 *Phys. Rev.* **75** 884
[47] Williams C D H and Wyatt A F G 2003 *Physica* B **329–333** 262